Proceedings of GT2006
ASME Turbo Expo 2006: Power for Land, Sea and Air
May 8-11, 2006, Barcelona, Spain

GT2006-90385

The Design, Analysis and Test of a Unique Gas Turbine Scroll for the F-35, Joint Strike Fighter

Hakan Aksoy, Stony W. Kujala, Craig W. McKeever, Ly D. Nguyen
Honeywell Engines, Systems & Services, P.O. Box 52181, Phoenix, Arizona 85072, USA

ABSTRACT

The design of the APU (Auxiliary Power Unit) for the F-35 JSF (Joint Strike Fighter) focused on minimizing size and weight while meeting stringent performance goals. To help realize that goal, a unique turbine scroll was designed. The scroll design delivers air from the combustor to the turbine inlet with minimal loss and flow distortion while minimizing design space.

CFD (Computational Fluid Dynamics) results of scroll total pressure loss and exit peripheral distribution of total pressure, Mach number, and flow angle are presented. Rig tests were utilized for measuring and validating the computed total pressure and Mach number distributions around the periphery of the scroll exit. Comparisons of the CFD simulations and test data indicate strong correlation in values of average total pressure loss, local total pressure loss and Mach number around the exit periphery.

NOMENCLATURE

A	Scroll cross sectional area
C	Velocity
K	Constant in Eq. (1)
$\dot{m}$	Mass flow rate
r	Radius
α	Flow angle
ρ	Density

Subscripts:

1	Scroll inlet location
2	Scroll exit location
m	Meridional component
θ	Peripheral location around scroll (0^o to 360^o)

INTRODUCTION

Gas turbine engine design has drastically improved with the use of digital technology in the last few decades. The technology improvement has particularly occurred in the areas of design, analysis and modeling. This improvement enables engineers to develop more compact and higher performance engines.

The design of the APU for the F-35 JSF engine meets stringent size, weight, and performance constraints. The scroll is one component that could affect the final size of the APU if it were not designed carefully. Therefore, its compact design and performance are important.

A methodology that outlines the important concerns in designing a radial turbine scroll is described in Baines [1,2]. Furthermore, Chapple et al. [9] provides additional background on scroll design approaches. A typical scroll is characterized by a circular inlet section, and a volute that is centered above the scroll exit. Its peripheral shape is defined by uniformly decreasing circular cross sections. However, unlike the typical scroll, the scroll presented here needed to be somewhat unusual in shape due to the space constraints imposed on the design.

The scroll is part of the combustion system that is shown in Fig. 1. Within this system, the air is fed from a can combustor that has a circular cross section. A transition duct provides the smooth transformation from the circular shape of the can combustor to the irregular shape at the scroll inlet section as shown in Figs. 2 and 3. Downstream of the scroll inlet, the cross section of the scroll continually changes in shape as it reduces in size around the periphery. In addition to this irregular change in shape, the present scroll exhibits a noted axial shift in cross section. Unlike the typical scroll that has its cross sectional centroids centered above its exit, this scroll starts with its sectional centroids on aft side of the

exit and, as one progresses around the periphery of the scroll, the cross sectional centroids shift axially to the front side of the exit. This unusual design was required to fit the scroll to the small space available within the combustion system. During the multiple iteration design phase, this axial shift was reduced from what is shown in Fig. 3 to that of Fig. 7 in the final design.

3D CAD modeling and viscous CFD analysis were used to expedite the optimized design of the scroll with low aerodynamic losses and uniform exit flow conditions. Rig testing verified the aerodynamic performance of the scroll by demonstrating low loss and uniform exit flow.

GENERAL DESIGN APPROACH

The primary design considerations for the turbine scroll include aerodynamic performance, occupied space, weight, cost, scroll cooling, and manufacturability. Stringent space limitations for the combustion system, shown in Fig. 1, were set by a maximum weight limit on the turbomachine. The scroll space limitations existed in both radial and axial directions. The combustor liner and the scroll needed to utilize the tight space in the combustion chamber without adversely jeopardizing the other requirements, especially aerodynamic performance.

Aerodynamic considerations required careful selection of cross-sectional area at the scroll inlet, cross-sectional area to centroid radius ratio (A/r) about the periphery of the scroll, combustor exit direction, and combustor to scroll transition.

The design of the scroll body began with the allowed space envelope, cross-sectional area at the scroll inlet, and linear A/r relationship between the cross-sections. Here, r is the radius to the centroid of a given cross section. The inlet cross-sectional area of the scroll was determined by the desired Mach number and its initial shape and centroid were defined. Referring to Fig. 2, a spiral spline, which passes through the centroid of each cross-sectional area, was used to guide the shape of the scroll. Creation of the spline is an important step in optimization of the scroll shape since it defines the orientation of the subsequent generating-curves for the irregular sections around the scroll periphery. The spline helps guide the generation of planar curves for scroll-surface creation as depicted in Fig. 2. Each irregular, cross-sectional curve is created in its own plane that is normal to the spline.

The above process assumes one dimensional flow since r is the radius to the area centroid, and not the radius to the 50% streamline. In other words, for a given scroll cross section, C_θ is assumed to be constant and indepentant of r. In reality, the actual value of r representing the 50% streamline will differ slightly from the assumption that it exists at the area centroid. However, in order to expedite the scroll design process whereby the scroll section areas are guided by the spiral spline, the simplified approach of using the area centroid was used. Based on the results of the CFD analysis and rig testing, it appears that this assumption was a justified simplification in designing a low loss scroll with reasonably uniform exit conditions around the periphery.

The transition duct delivers the air from the circular cross section of the combustor exit to the non-circular cross section of the scroll inlet. A gradual change in shape of this duct was desired because poor flow conditions at the exit of the transition duct translate into non-uniform flow and losses around the periphery of the scroll exit. However, the space constraints set the length of the transition duct to be shorter than initially desired. To provide a smooth, gradual change in shape, within a short distance, required multiple iterations of the transition duct / scroll body system. Early in the design phase, a scroll shape was proposed that had a significant axial shift in the scroll body as shown in Fig. 3. However, it was also discovered through analysis that large axial shifts in the scroll body are also undesirable and lead to non-uniform flow conditions at the scroll exit. The final transition duct/scroll body system resulted from multiple iterations to find the optimal combination of shape change in the transition duct and reduced axial shift in the scroll body (Figs. 6-7). Fast turn around of the design iterations was achieved by use of the spiral spline method described in the above paragraph.

GENERAL ANALYSIS APPROACH

The function of the scroll is to deliver the air from the can combustor to the radial turbine as uniformly as possible and achieve this with minimal total pressure loss.

The combustion gases enter the scroll in a direction which is tangential with respect to the engine axis and are distributed around the periphery of the scroll radially inward towards the turbine nozzle. Flow that sweeps around the scroll upstream of the nozzle must re-enter and mix with the mainstream flow at the tongue of the scroll. A schematic of the scroll is shown in Fig. 4.

The principal design parameter is the inlet cross-sectional area to centroid radius ratio, A/r, which determines the angle of flow at exit of the scroll. This is also the angle at which the flow approaches the downstream nozzle. The scroll is defined on a series of cross sections about the periphery of the turbine. The critical parameters, cross-sectional area and the centroid radius of each section, must be carefully controlled if the flow is to be uniformly distributed as it enters the radial turbine.

Following the methodology described in references [1] and [2], a simple, ideal model of the flow in a scroll can be developed to establish the overall dimensions of a scroll in the following manner. Referring to Fig. 4 for nomenclature and assuming a constant angular momentum or free vortex flow inside the scroll, one can write:

$$r_\theta C_\theta = \text{cons tan t} = K \quad (1)$$

Also, the conservation of mass through any cross sectional plane at peripheral location θ gives:

$$\dot{m}_\theta = \rho_\theta A_\theta C_\theta \quad (2)$$

In these equations, C_θ is the local tangential component of velocity and $\dot{m}_\theta$ and ρ_θ are the local mass flow rate and density at a given θ location. A uniform mass distribution around the scroll is achieved when:

$$\dot{m}_\theta = \dot{m}\left(1 - \frac{\theta}{2\pi}\right) \quad (3)$$

Where $\dot{m}$ is the total mass flow rate at the scroll inlet. From these equations it can be shown that

$$\frac{A_\theta}{r_\theta} = \frac{\dot{m}}{\rho_\theta}\frac{1}{K}\left(1 - \frac{\theta}{2\pi}\right) \quad (4)$$

Therefore, for small variations in density, A_θ / r_θ must be a linear function of the peripheral angle in order achieve a uniform mass flow distribution around the scroll.

The scroll exit flow angle α_2, is defined as:

$$\tan\alpha_2 = \frac{C_{\theta 2}}{C_{m2}} \quad (5)$$

where C_{m2} is the meridional component of the velocity vector. Substituting the tangential component of the velocity from the free vortex equation and the meridional component from the continuity equation into Eq. (5), one can show that

$$\tan\alpha_2 = \frac{\rho_2}{\rho_1}\left(\frac{A_2/r_2}{A_1/r_1}\right) \quad (6)$$

Hence, for small changes in density, the flow angle at the inlet to the radial turbine is a function of the scroll exit to inlet A/r ratio. Using this method, excellent agreement was observed between the scroll exit flow angle computed from Eq. (6) and the mass-averaged value obtained from the CFD analysis.

Normally, the scroll exit dimensions would be fixed by the design of the radial nozzle, therefore, Eq. (6) implies that the exit flow angle is determined solely by the choice of the inlet cross-sectional area and radius. Equations (4) and (6) also give us some simple design rules for scrolls:

1. The value of A/r for each peripheral section must decrease linearly with azimuthal angle for uniform exit conditions and
2. The choice of A/r at the inlet determines the scroll exit flow angle.

Besides these, there are other guidelines that the designer needs to be aware of in designing a scroll. One of these is to maintain a reasonably low Mach number within the scroll so that the losses can be controlled without difficulty. Another requirement is to design the scroll surface area small enough so that it can be cooled effectively with the limited amount of cooling flow available.

Trade-off studies were carried out on multiple scroll geometries that were proposed and analyzed during the design process. However, here the results are presented from the CFD analysis of the best performing scroll with explanations of the improvements over the earlier iterations.

Figure 5 shows that a linear A/r distribution was maintained by the present scroll to provide a uniform flow distribution to the turbine. The scroll body inlet area of the first iteration scroll that was studied was later found to be too large to cool with the amount of cooling flow available. Therefore, the inlet area was reduced in the subsequent designs.

Figures 6 through 8 show various views of the scroll and point out the geometric characteristics that might lead to a non-uniform scroll exit flow and higher scroll losses. In general, the transition duct should deliver the flow from the combustor to the scroll as tangentially as possible as shown in Fig. 6. If this flow has strong axial or radial components to it, then one can expect the flow at the scroll exit to be less uniform in the critical region where the scroll inlet plane and tongue meet. Attention was also paid to the transition of the duct from the combustor to the scroll inlet in order to avoid introducing a diffusing duct that could cause the flow to separate resulting in increased losses.

Also, presence of large dumps (backsteps) where the transition duct meets the scroll inlet plane are considered undesirable as they would lead to regions of flow recirculations near the tongue and would contribute to the scroll losses and the unevenness in the scroll exit flow. Fig. 8 shows the amount of dump at the scroll inlet plane.

Scroll boundary conditions were specified based on the engine cycle conditions at the design point. This cycle point was simulated using the NUMECA International's Fine/Turbo CFD code with the Baldwin-Lomax algebraic turbulence model [3]. It should be noted that some past studies have utilized inviscid codes successfully in

designing well performing scrolls [4-7]. However, the use of a viscous solver allows the computation of the scroll total pressure loss and the comparison of various scroll designs to help with the selection of the best performing scroll. Also, Baldwin-Lomax model allows prediction of the three dimensional viscous effects with minimal computational effort within a tight design schedule when compared with more elaborate two equation turbulence models. It was believed that this turbulence model would be sufficient for the present, primarily circumferential flow that does not exhibit strong, adverse pressure gradients and associated flow separation. Additionally, present study was more interested in the relative levels of total pressure loss from one design to another rather than the absolute levels. It should however be mentioned here that predicted and measured total pressure losses were indeed in good agreement with each other as it will be explained in the following section.

By adopting "Butterfly" type mesh with IGG (Fine/Turbo's mesher) a sufficiently orthogonal mesh could be generated with 1,184,400 nodes as shown in Figs. 9 through 11.

Normalized Mach number distributions are shown around the scroll exit plane at 10, 50, and 90% spans from hub-line to shroud-line of the turbine flowpath in Fig. 12. The Mach number is normalized by the average exit Mach number. The present scroll showed a more uniform Mach number distribution than the other design iterations that were analyzed during the design cycle. Figs. 13 and 14 show the pathlines to explain the importance of the transition duct design. If the transition duct does not deliver the flow tangentially (with respect to the engine axis), too much of the gas exits the scroll too soon and we see a non-uniform flow distribution in Fig. 15 just downstream of the scroll inlet. As seen from these figures, this leads to regions of high mass flux (dark blue regions in Fig. 13) near the endwall. This in turn results in low flow angles in Fig. 16 near the hub-line endwall regions as a result of low tangential component of the velocity. Otherwise, the scroll exhibits a rather uniform flow angle at 50 and 90% span. Some of the flow that circulates inside the present scroll re-enters from the tongue as seen in Fig. 14 as red pathlines.

Spanwise area-averaged plots of flow angle and Mach number shown in Figs. 17 and 18 indicate that, in general, the scroll delivers a uniform flow.

The CFD results also indicated that the total-to-total pressure loss of the final scroll was within the design requirements. The final iteration scroll pressure loss was reduced by approximately 30% with respect to the first iteration scroll.

Therefore, based on the results described above, this scroll was accepted as the turbine scroll.

It should also be mentioned that, early in the design process, the CFD simulations were also carried out with the radial nozzle downstream of the scroll. The mesh used for this extended model is shown in Fig. 19. When the combined scroll and the nozzle model was run, a fully-nonmatching mesh boundary (FNMB) condition was used to transfer the flow information from the nodes on the scroll exit patch to the nodes on the nozzle inlet patch. Since the tangential distribution of the nodes on the scroll exit patch was significantly coarser (which was later refined) than those on the nozzle inlet patch (which needed to be clustered due to the presence of solid boundaries of the airfoils), the computed flow variables were seen to show unsteadiness at this interface. However, the general trends of the profiles of all variables closely followed those obtained from the scroll only analysis. Therefore, in the subsequent analysis of the scroll design iterations, the nozzle assembly was not included in the CFD models to shorten the computational time and storage.

Plots in Figs. 20 and 21 from the combined scroll/nozzle analysis show that the mass flow is uniformly distributed to the individual nozzle passages and that the presence of the nozzle smoothens out the uneven flow significantly at the rotor inlet plane. In Fig. 20, $\dot{m}_i$ is the mass flow rate in a given passage of the nozzle and it is normalized by the ratio of total mass flow rate at the scroll inlet to number of vanes which is 27.

TEST RESULTS AND VALIDATION

Testing of the turbine scroll was carried out to verify the scroll CFD analysis and scroll performance. Overall average scroll total pressure loss was measured, as well as uniformity in scroll exit loss and Mach number around the periphery of the scroll.

The transition duct inlet was fed by conditioning the flow by first passing it through a pressure drop screen and straightening tubes. This was done to ensure uniform inlet conditions and the ability to obtain accurate measurement of total pressure at the inlet. Mass flow was measured by an orifice plate located upstream of the scroll.

The scroll exit conditions were measured by a rake of total pressure probes mounted to a rotating drum. Four spanwise total pressure probes were mounted to the rake. Static pressure taps were also installed in the rotating drum. The peripheral distribution of scroll exit total pressure and static pressure was measured by rotating the drum in increments of 2 degrees.

Fig. 22 shows a cross section of the test rig. Fig. 23 shows a photo of the scroll exit instrumentation drum and the location of the instrumentation.

The test results indicated the scroll 1D average total pressure loss, as well as the peripheral distribution of total pressure loss to be in close agreement with the

CFD analysis result. Figure 24 shows the peripheral distribution of total pressure loss. The loss is based on the spanwise average of the scroll exit total pressure probes in relation to the scroll inlet average total pressure. The CFD and test data agree well with each other. In particular, the spike in loss due to the scroll tongue is captured very well by both the CFD and test. The peripheral location of the spike as well as the width of the spike, are comparable. The CFD solution does not capture the full amplitude of the loss spike, which may be due to numerical smearing from the density of the grid used in the region of the tongue. A spike in total pressure loss in the tongue region is typical of turbine scroll design. The interested reader is directed to Scrimshaw et al. [10] and Miller et al. [8] for other examples of scroll designs and test results showing scroll total pressure loss with a localized spike in total pressure loss near the tongue.

Figure 25 shows the peripheral distribution of normalized Mach number. The Mach number is calculated based on the spanwise average of total pressure at a given peripheral location at the scroll exit, in conjunction with the local static pressure at that location. The normalized Mach number is calculated by dividing the local Mach number by the 1D average exit Mach number. The test data and CFD results of scroll exit Mach number are seen to agree well. A uniform distribution of exit Mach number is illustrated with a local deficit in Mach number in the location of the tongue.

The relatively uniform distribution of loss, as well as the fact that the spike in loss is confined to a minimal peripheral distance is indication that the scroll is performing well aerodynamically. The uniform exit Mach number distribution, as well as the overall 1D average loss also verifies the aerodynamic design of the scroll.

Attention to detail in carefully selecting the scroll cross section shape distribution, transition duct shape and design of the tongue has resulted in a scroll that performs well, and meets the small space constraints imposed by the engine configuration.

CONCLUSIONS

A turbine scroll was successfully designed using state-of-the art CAD and viscous CFD tools and analysis techniques following the general scroll design practices. Despite severely limited space for the scroll and weight restriction, the current scroll showed low levels of total pressure loss and uniform flow exit conditions as verified by both the CFD predictions and test results.

A butterfly type mesh and utilization of fully-nonmatching mesh boundaries were found to be very efficient for the CFD analysis of the present scroll that has cross sections that are significantly non-circular.

CFD analysis was carried out with and without the presence of the radial nozzle downstream of the scroll. Strong similarity in the results from the two runs indicated that, for most practical purposes, this scroll could be analyzed without including the downstream nozzle in the model. It was also seen that the presence of the nozzle helps to introduce a more uniform flow to the turbine rotor.

Good agreement was seen in the measured and predicted values of total pressure loss and Mach number distributions around the periphery of the scroll exit.

ACKNOWLEDGEMENTS

The authors would like to thank Lockheed Martin and Honeywell for their support in bringing this paper to publication. NUMECA International is also recognized for their advice on the CFD modeling.

REFERENCES

[1] Baines, N. C., 1997, “The Aerodynamics of Radial Turbines,” *Notes by Concepts ETI, Inc*., Wilder, VT, USA.
[2] Baines, N. C., 1997, “Radial Turbine Design,” *Notes by Concepts ETI, Inc*., Wilder, VT, USA.
[3] Baldwin, B. S. and Lomax, H., 1978, “Thin Layer Approximation and Algebraic Model for Separated Turbulent Flows,” *AIAA-78-257.*
[4] Hamed, A., Baskharone, E. and Tabakof, W., 1978, “A Flow Study in Radial Inflow Turbine Scroll-Nozzle Assembly,” *J. Fluids Engineering*, Vol 100, pp. 31-36.
[5] Hamed, A., Abdallah, S., and Tabakoff, W., 1977, “Flow Study in the Cross Sectional Planes of a Turbine Scroll,” *AIAA-77-714*.
[6] Hamed, A., Abdallah, S., and Tabakoff, W., 1978, “Computer Program for the Analysis of the Cross Flow in a Radial Inflow Turbine Scroll,” *NASA-CR-135321*.
[7] Lymberopoulos, N., Baines, N. C., and Watson, N., 1988, “Flow in Single and Twin Entry Radial Turbine Volutes,” *ASME Paper No. 88-GT-59*.
[8] Miller, E. C., L’Ecuyer M. R. and Benisek, E. F., 1987, “Flowfield Surveys at the Rotor Inlet of a Radial Inflow Turbine,” *ASME Paper No. 87-ICE-52*.
[9] Chapple, P. M., Flynn, P. F. and Mulloy, J. M., 1980, “Aerodynamic Design of Fixed and Variable Geometry Nozzleless Turbine Castings,” J. Engineering for Power, Vol. 102, pp. 141-147.
[10] Scrimshaw, K. H. and Williams, T. J., 1984, “Size Effects in Small Radial Turbine,” ASME Paper No. 84-GI-215.

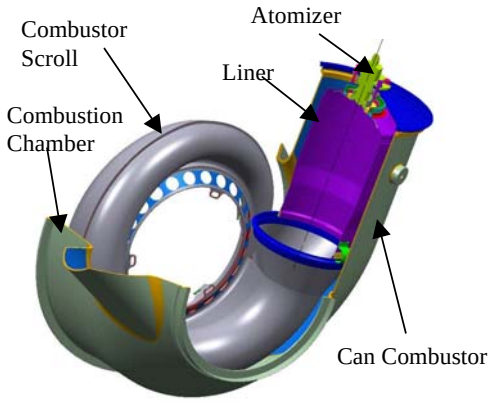

Figure 1. Combustion system.

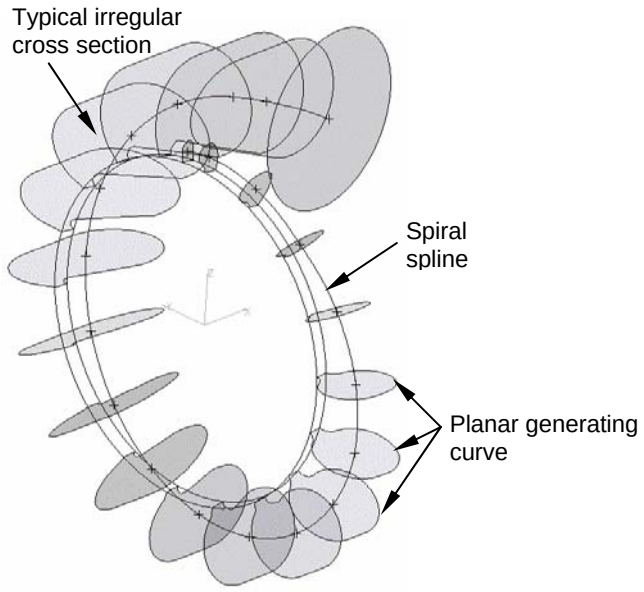

Figure 2. Spline modeling concept utilizing CATIA.

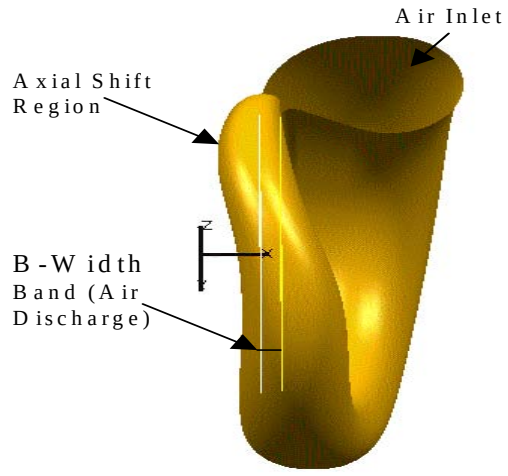

Figure 3. 3D scroll body surface with axial shift (this scroll was not adopted due to high axial shift and loss).

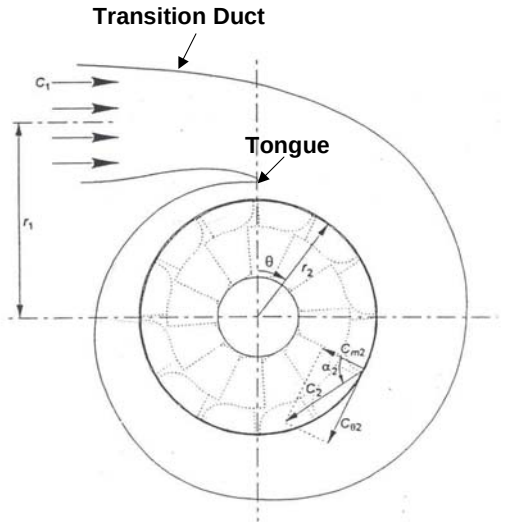

Figure 4. A two-dimensional schematic of the radial turbine scroll (sketch taken from [1]).

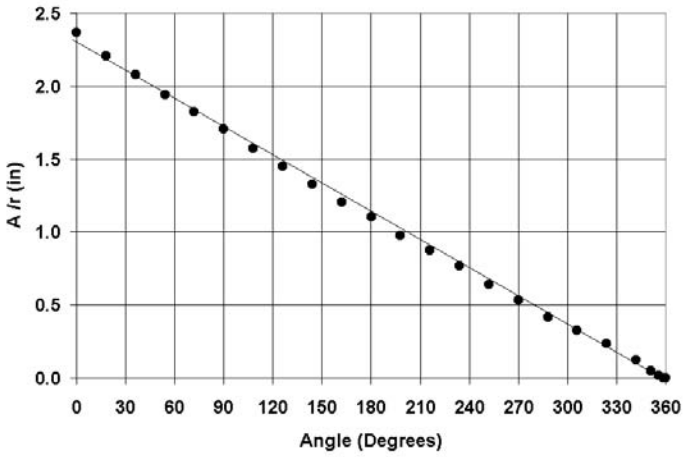

Figure 5. A/r distribution.

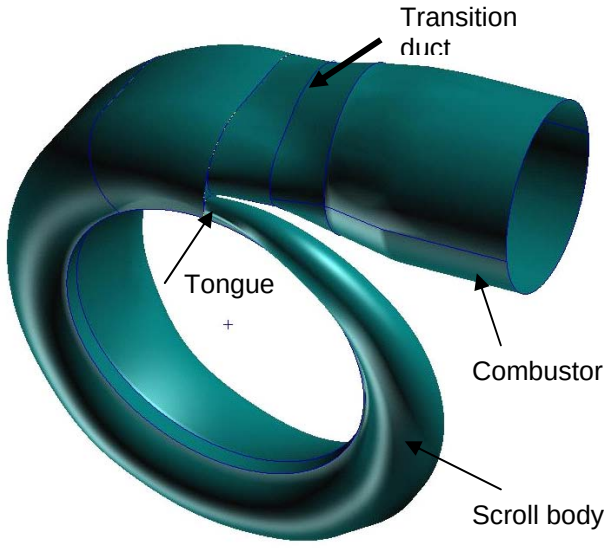

Figure 6. Scroll with its improved transition duct.

Figure 7. The amount of axial shift was minimized during the design process of the scroll.

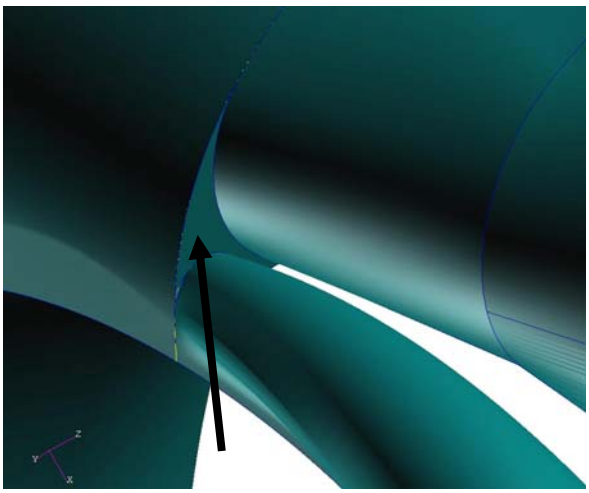

Figure 8. The amount of dump (back-step) region (shown with an arrow) was minimized during the design process of the scroll.

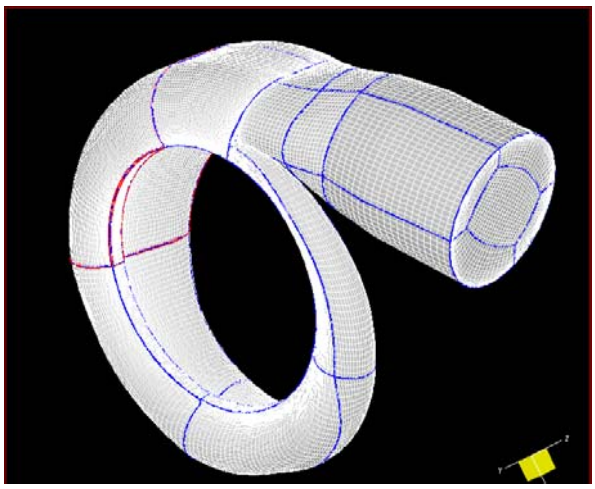

Figure 9. Structured mesh was adopted for the whole scroll.

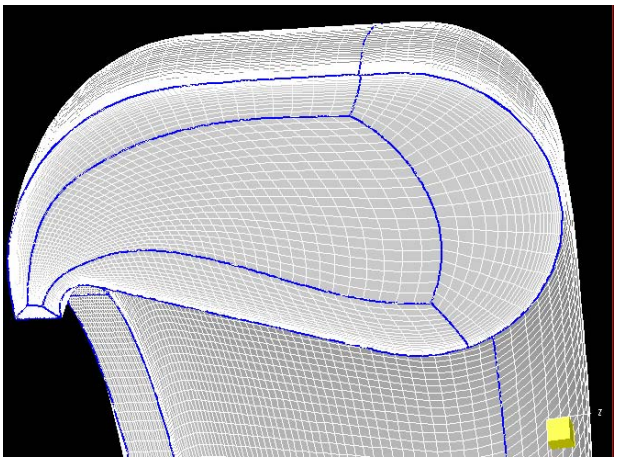

Figure 10. Structured butterfly mesh at the scroll inlet.

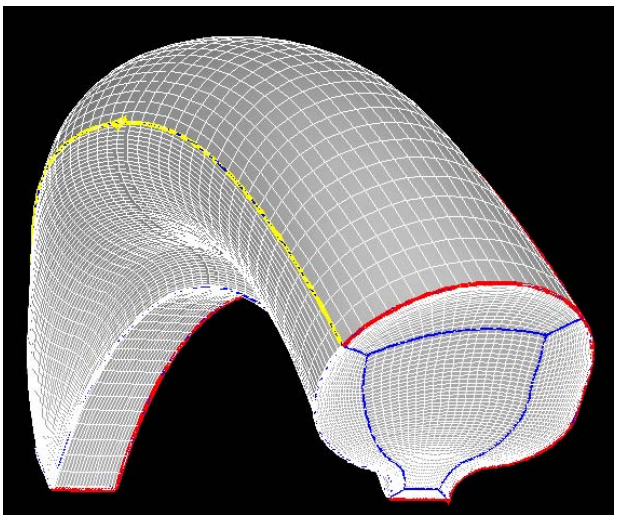

Figure 11. Structured butterfly mesh used for the blocks that define the tongue area of the scroll.

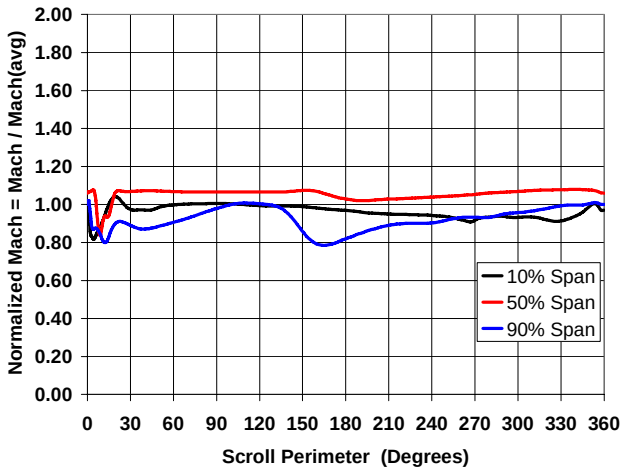

Figure 12. Scroll exit normalized Mach number distribution. (local exit Mach number / 1D average exit Mach number).

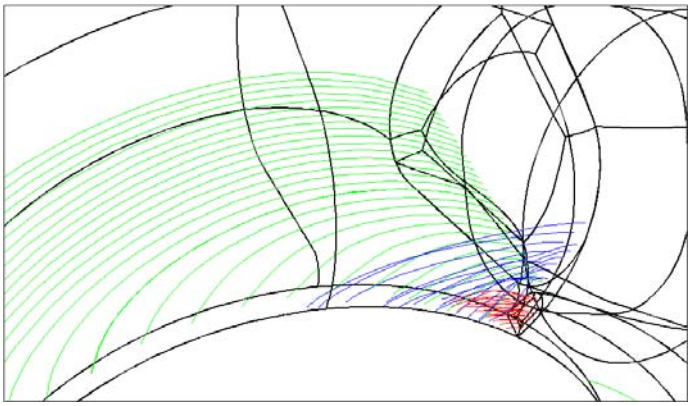

Figure 13. Pathlines (scroll exit plane contours colored by radial mass flux).

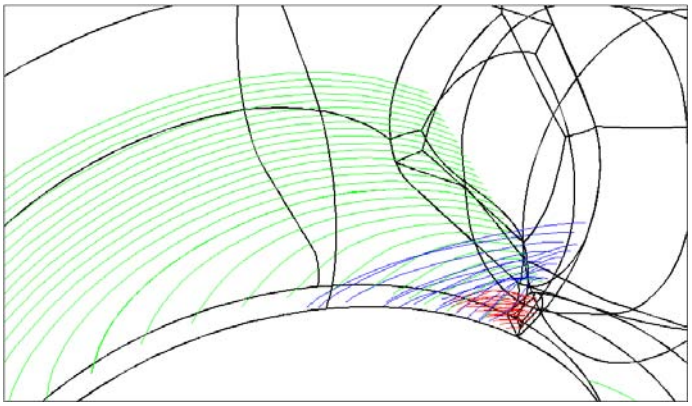

Figure 14. Pathlines showing some re-entering flow from the tongue (shown in red).

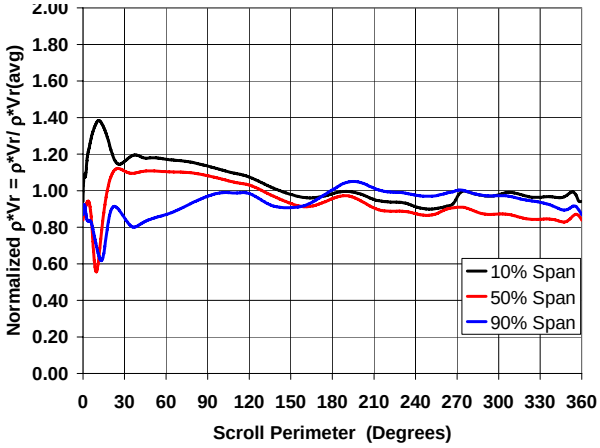

Figure 15. Scroll exit radial mass flux distribution normalized by exit 1D average radial mass flux.

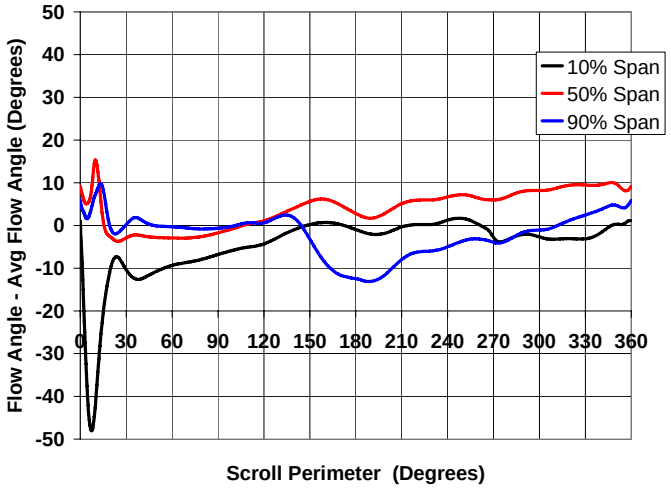

Figure 16. Scroll exit flow angle distribution. (Local flow angle minus 1D average flow angle at scroll exit).

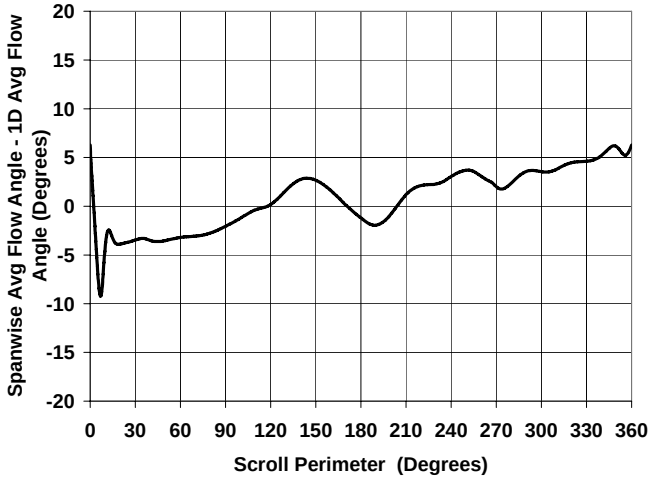

Figure 17. Spanwise averaged flow angle distribution minus 1D average flow angle at the scroll exit.

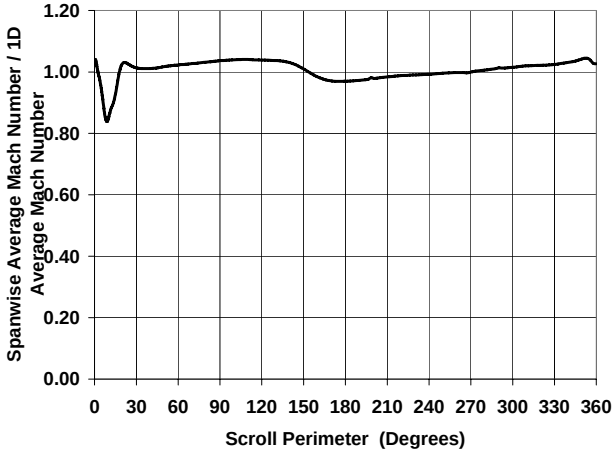

Figure 18. Spanwise averaged Mach number distribution normalized by 1D average Mach number at the scroll exit.

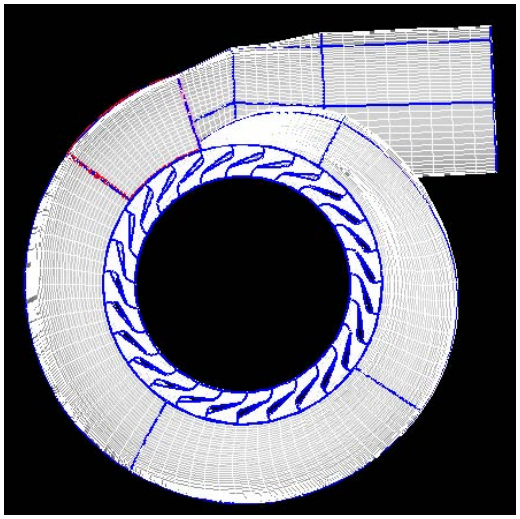

Figure 19. Mesh used for combined scroll and nozzle analysis (with the first scroll early in design process).

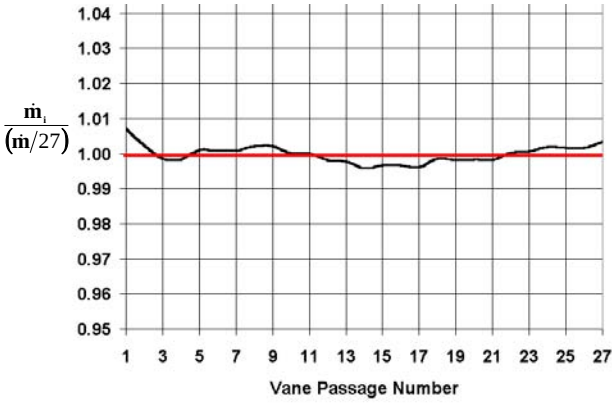

Figure 20. Mass flow through individual passages of the nozzle (vane count is 27).

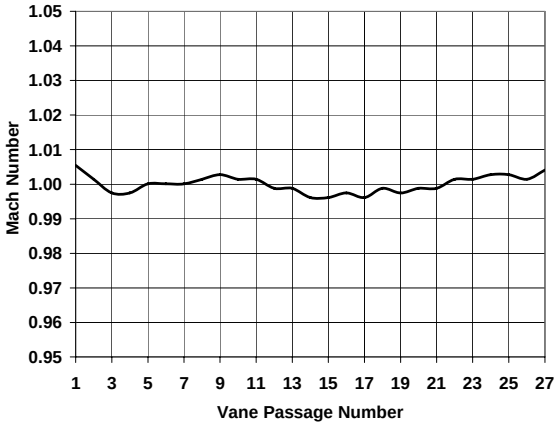

Figure 21. Normalized Mach number at the exit of the nozzle assembly.

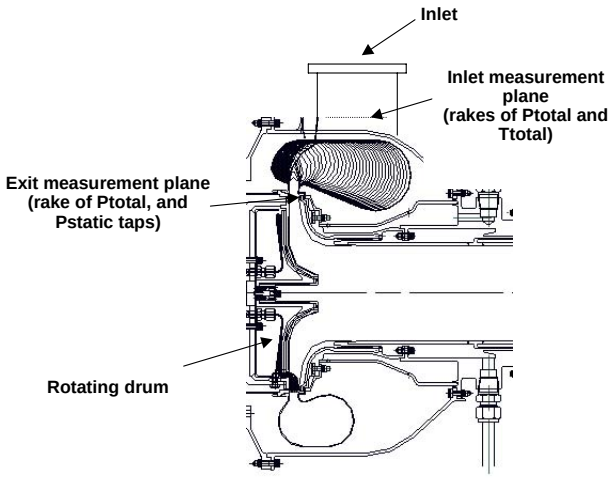

Figure 22. Cross section of scroll test rig.

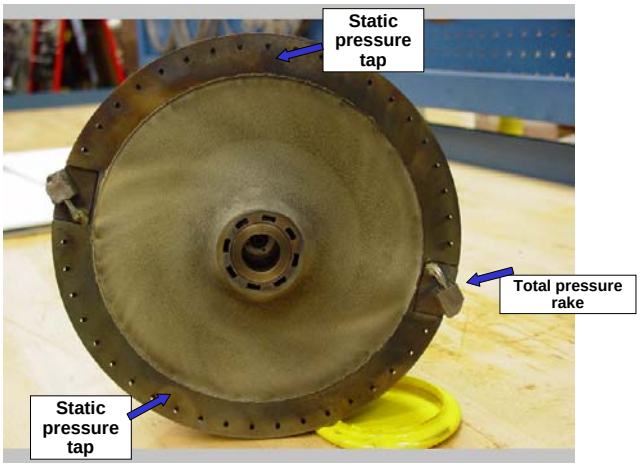

Figure 23. Photo of rotating drum with instrumentation rake and static pressure taps.

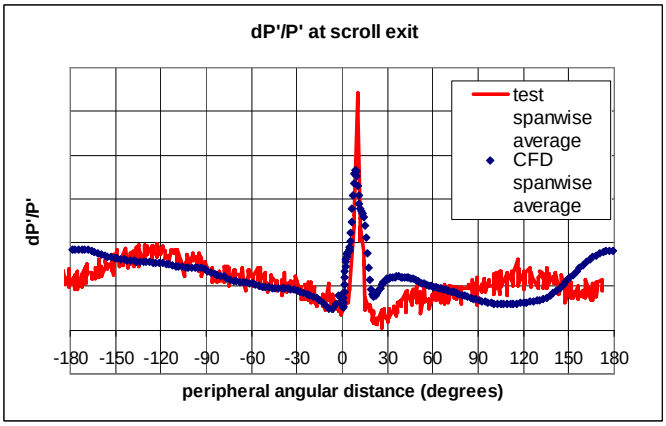

Figure 24. Scroll total pressure loss based on exit spanwise average total pressure and average inlet total pressure.

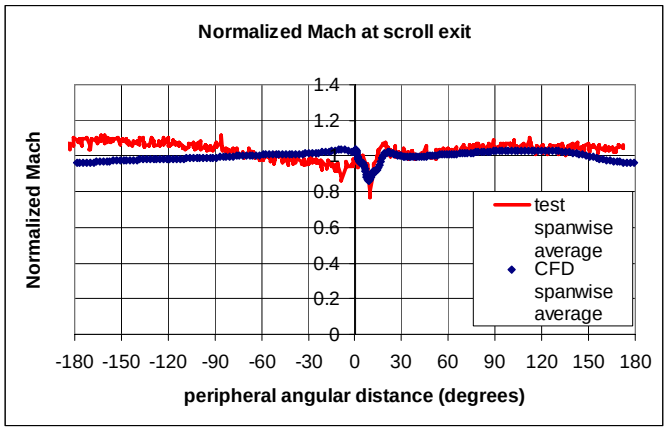

Figure 25. Scroll exit normalized Mach number (exit spanwise average Mach number / exit 1D average Mach number).